Influence of an upper layer liquid on the phenomena and cavity formation associated with the entry of solid spheres into a stratified, two-layer system of immiscible liquids

Tan, B. & Thomas, P.

DOI 10.1063/1.5027814
ISSN 1070-6631
ESSN 1089-7666
Publisher: AIP Publishing

Influence of an upper layer liquid on the phenomena and cavity formation associated with the entry of solid spheres into a stratified, two-layer system of immiscible liquids

Benedict C.-W. Tan[1,2*] and Peter J. Thomas[1]

[1]Fluid Dynamics Research Centre, School of Engineering, University of Warwick, Coventry CV4 7AL, UK

[2]School of Mechanical, Aerospace and Automotive Engineering, Coventry University, Coventry CV1 5FB, UK

Abstract: New phenomena not previously documented in the available literature have been experimentally observed subsequent to the entry of falling steel spheres into a stratified system of a shallow layer of sunflower oil above a deep pool of water. Further experiments on similar sphere entries into sunflower oil demonstrated that those phenomena arose mainly as a result of the interaction between the surface of the spheres and the sunflower oil. It should be noted that the sunflower oil layer in the aforementioned two-layer system was relatively very thin compared to the dimensions of the spheres. Therefore, the experiments showed the substantial influence both the upper layer liquid and the surface conditions of the solid body could potentially have, on the phenomena and cavity dynamics that arise as a result of solid entries into stratified, two-layer systems of immiscible liquids.

1. Introduction

The entry of solid bodies into water and their associated phenomena have long fascinated mankind. Modern systematic and scientific studies on the subject have their origins from the pioneering work of Worthington (1882, 1908) and Worthington & Cole (1897, 1900).

In the classic scenario, a solid body possessing appropriate surface conditions and sufficient impact velocity, generates a cavity at its wake subsequent to its entry into water or other liquids. The cavity expands while connecting the solid body to the liquid surface prior to a pinch-off arising from the combined influence of hydrostatic pressure, atmospheric pressure and surface tension forces. This pinch-off splits the cavity into two and the process is known in the literature as the 'deep seal' as it occurs at a significant depth below the liquid surface as compared to other cavity sealing phenomena. The upper cavity collapses rapidly towards the liquid surface, generating an upward jet commonly known as the *Worthington jet*. Meanwhile, the lower cavity remains attached to the solid body and may experience further pinch-offs, splitting into multiple smaller cavities.

In addition to the deep seal, the literature also identifies two other types of significant cavity pinch-offs – 'surface seal' and 'shallow seal'. A surface seal normally occurs after a high solid body with high inertia enters into a liquid. As a result of a combination of aerodynamic pressure and Laplace pressure, a splash crown is forced to dome over the cavity, effectively sealing it as described by Aristoff & Bush (2009), and Truscott *et al.* (2014). Meanwhile, shallow seal occurs almost immediately after liquid entry by a solid with low inertia as the relatively small cavity experiences a pinch-off close to the liquid surface. The main difference between a shallow seal and a deep seal is that the former is a consequence of capillary instability while the latter occurs as a result of the combined influences of hydrostatic pressure, aerodynamic pressure and surface tension. However, the shallow seal and deep seal have similar appearance and according to Truscott *et al.* (2014), a jet would also be generated subsequent to shallow seal.

The practical applications and potential benefits to the military as shown by May (1951, 1952) in addition to the continued interests in the subject have maintained the popularity of solid-liquid entry studies to this day. Advances in science and technology have allowed modern physicists and engineers to study the cavity dynamics computationally in greater details as demonstrated by, for instance, Gekle *et al.* (2009, 2010, 2011), Gekle & Gordillo (2010), Gordillo & Gekle (2010), Lee *et al.* (1997), and Peters *et al.* (2013). In recent years, studies have also involved liquids other than water, for instance, Le Goff *et al.* (2013) used oil while Akers & Belmonte (2006) used viscoelastic miscellar fluid.

As a result of over a century of detailed study, the cavity dynamics and phenomena associated with the entry of solid bodies into single-phase, homogeneous liquids are well-known and have been widely documented in literature.

However, the same amount of knowledge and understanding does not exist for the corresponding entry into stratified, two-layer systems of immiscible liquids (eg. water filled with a thin layer of oil). There is relatively little amount of literature on such study prior to the recent works of Tan (2016) and Tan *et al.* (2016) that show the formation of wave-like instability along the cavity walls behind the steel spheres. Further analysis showed that these instabilities were caused by the shear between the upper and lower layer liquids involved in the experiments. Meanwhile, it is worth noting that Franklin (1774) as early as in the 18th century, had observed from on board a ship the stilling of waves subsequent to the cooks pouring oil into the sea. Therefore, it can be concluded that even a thin oil layer would potentially have significant influence on the dynamics of the water that is directly underneath it.

2. The Experiments

The experiments involved releasing solid spheres from variable heights, 0.1 m $\leq h \leq$ 1.8 m for the generation of different impact velocities, 1.4 m/s $\leq u_i \leq$ 5.94 m/s, into a large tank filled with the liquids used in the present study.

The set-up involved a large tank filled with either water, sunflower oil or a combination of both. The depth of the liquids and the width of the tank were set at above 20 times the diameter of the largest spheres used in the experiments in an effort to minimise wall effects. The sunflower oil had a density, $\rho_o = 920$ kg/m^3, kinematic viscosity, $\nu_o = 54$ mm^2/s and surface tension, $\sigma = 0.0337$ kg/s^2. The water used was British tap water which had a density, $\rho_w \approx 1000$ kg/m^3 and kinematic viscosity, $\nu_w = 1$ mm^2/s. The spheres were AISI Chrome 52100 stainless steel ball bearings that had density, $\rho_s = 7800$ kg/m^3 and diameters 2.9 mm $\leq D \leq$ 14.3 mm. Steel spheres were chosen to minimise buoyancy effects.

The spheres were released using an electromagnet while a high speed camera (Phantom 5.2) with a frame rate up to 2900 frames per second was used to record and analyse the entire sphere entry process. Meanwhile, throughout the experiments, room temperature was kept constant at 21^{o}C by an air conditioner in an endeavour to minimise temperature-induced viscosity variations in the liquids involved.

3. Results

3.1. Cavity sealing phenomena for two-layer sunflower oil-water experiments

Figure 8 of Aristoff & Bush (2009) presents a regime diagram showing the four different cavity sealing phenomena observed subsequent to the entry of solid spheres into water with respect to the Bond number, $Bo = \rho g R^2/\sigma$ and the Weber number, $We = \rho u^2 R/\sigma$ where R and σ represent the sphere radius and the surface tension of water respectively. Therefore, one could interpret from the figure that should all other qualities remain constant, quasi-static seal, shallow seal, deep seal and surface seal would be observed in increasing order of impact velocity.

However, this order of phenomena appeared to be different when steel spheres entered into a two-layer sunflower oil-water system. In addition to the deep seal, shallow seal had also been observed as the sphere entered with relatively high impact velocity. Further increases in impact velocity would result in the deep seal not occurring completely with the sphere experiencing only shallow seal that occurred almost immediately after its entry into the liquids.

Figures 1 to 4 display photographs illustrating the various flow phenomena generated by steel spheres following their entry into a two-layer, sunflower oil-water system, in the order of increasing impact velocity. Note that the diameter of the sphere visible in each figure is provided in the figure descriptions which provides a scale reference. Video recordings also revealed that the spheres could leave an ‘oil trail’ behind them and shed parts of their cavities in the form of vortex clouds that consisted of mixtures of oil droplets and air bubbles. Therefore, as shown in Figures 3 and 4, a small region of emulsion could be found at the wake of the sphere during this process.

The shallow seal transition velocity, u_{ss} is defined as the impact velocity of the sphere above which the 'unusual' shallow seal appears as shown in Figures 2, 3 and 4. Multiple repeated experiments confirmed the value of u_{ss} for steel spheres of every diameter used in the present study. It was found that u_{ss} generally decreased with increases in sphere diameter and this result suggests that the occurrence of the shallow seal is dependent on the inertia of the solid body. Figure 5 presents a regime diagram that shows the generation of shallow seal with respect to the Bond number, $Bo = \rho_o g D^2/\sigma$ and Weber number, $We = \rho_o u_{ss}^2 D/\sigma$ of the sunflower oil.

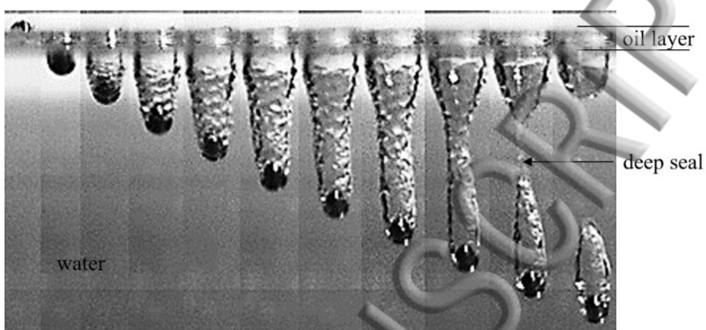

Figure 1: A modified version of Figure 21 from Tan (2016). The entry of a steel sphere (D = 10 mm and u_i = 2.43 m/s) into a deep pool of water with a 5 mm sunflower oil layer on its surface. Only the deep seal has been observed in this figure. The time difference between each successive image is 5 ms.

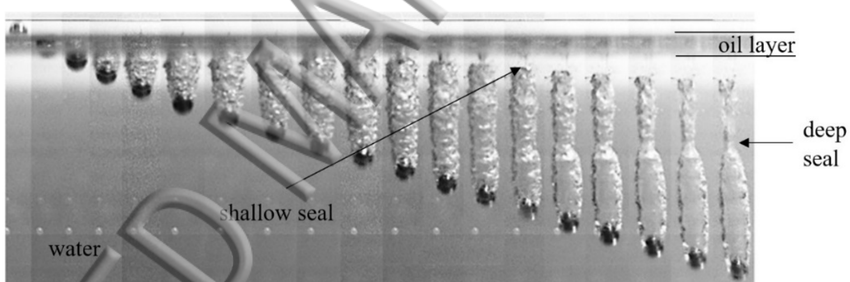

Figure 2: A modified version of Figure 22 from Tan (2016). The entry of a steel sphere (D = 10 mm and u_i = 3.96 m/s) into a deep pool of water with a 5 mm sunflower oil layer on its surface. Shallow seal was observed close to the oil-water interface while deep seal was observed to occur slightly differently to that shown in Figure 1. The time difference between each successive image is 2 ms.

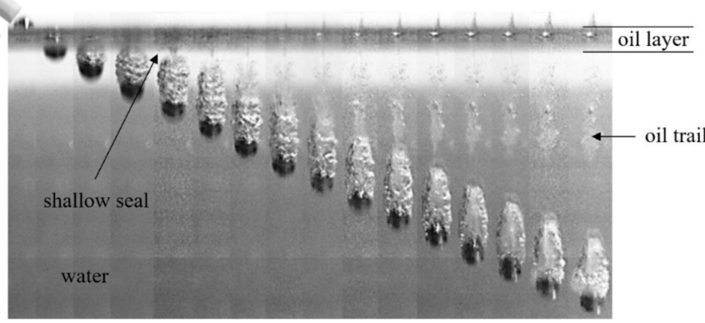

Figure 3: A modified version of Figure 23 from Tan (2016). The entry of a steel sphere (D = 10 mm and u_i = 4.85 m/s) into a deep pool of water with a 5 mm sunflower oil layer. Shallow seal occurred

close to the oil-water interface about 10 ms after sphere entry. It was observed that instead of an obvious deep seal as shown in Figure 1, the cavity left a trail of oil at its wake. The time difference between each successive image is 2 ms.

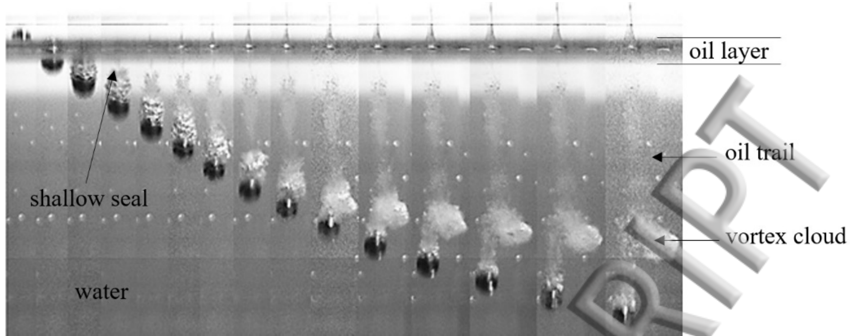

Figure 4: A modified version of Figure 24 from Tan (2016). The entry of a steel sphere (D = 10 mm and u_i = 5.6 m/s) into a deep pool of water with a 5 mm sunflower oil layer. Deep seal did not occur and a vortex cloud that consisted of a mixture of air-oil bubbles was generated at the wake of the sphere, creating a small region of emulsion. The time difference between each successive image is 2 ms.

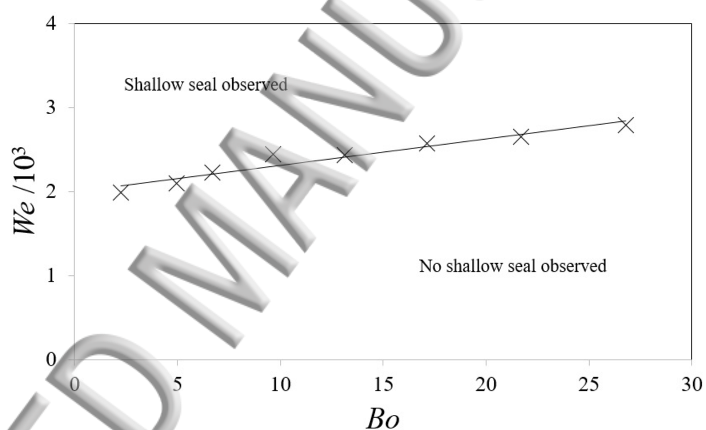

Figure 5: A regime diagram showing the occurrence of shallow seal with respect to the Bond number, *Bo* and Weber number, *We*. The shallow seal transition velocity, u_{ss} was found to be dependent on the sphere diameter, suggesting a relationship between the generation of the shallow seal and the sphere inertia.

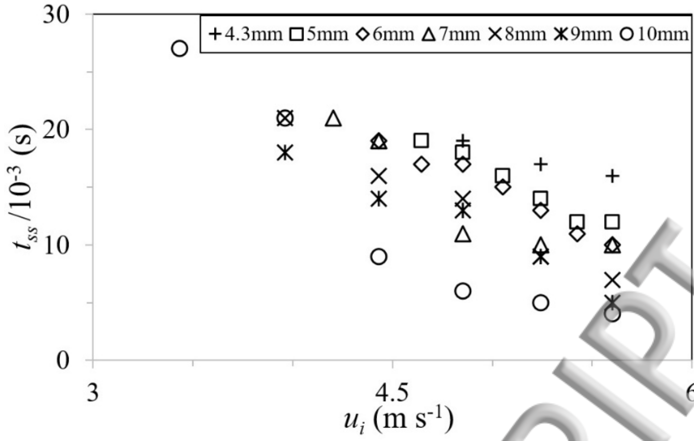

Figure 6: The shallow seal time, t_{ss} as a function of the impact velocities, u_i for spheres of various diameters as indicated in the legend.

Meanwhile, the shallow seal time, t_{ss}, is defined as the time interval between the instant of sphere entry into the two-layer, sunflower oil-water system and the instant when the aforementioned shallow seal occurs. The results shown in Figure 6 suggest that the cavity collapsed more rapidly for larger spheres and also for spheres that possessed higher impact velocity, u_i, demonstrating the dependence of t_{ss} on the sphere inertia. A consequence of the relatively short t_{ss} for larger spheres is the formation of smaller cavities as shown in Figures 3 and 4.

3.2. Cavity sealing phenomena for single-phase, homogeneous sunflower oil experiments

The phenomena documented in Section 3.1 was not known to exist during corresponding experiments involving water only. Similar sphere water-entry experiments performed during the present study confirmed that observation.

Therefore, it is reasonable to suggest that those phenomena in Section 3.1 might originate from the sunflower oil layer. In order to verify this hypothesis, a series of similar experiments involving the same steel spheres were performed using only sunflower oil. Figures 7 to 10 present the general cavity sealing phenomena observed during these entries.

Figure 7 presents the cavity generated at the wake of the sphere experiencing only the classic deep seal while Figure 8 shows the cavity experiencing both the deep seal and the shallow seal. It was found that above a certain impact velocity, the deep seal stopped occurring completely and as presented in Figures 9 and 10, the cavity experienced only shallow seal. As shallow seal occurred earlier in Figure 10, the cavity in the same figure was smaller than that in Figure 9. It has also been observed that surface seal did not occur when shallow seal was generated.

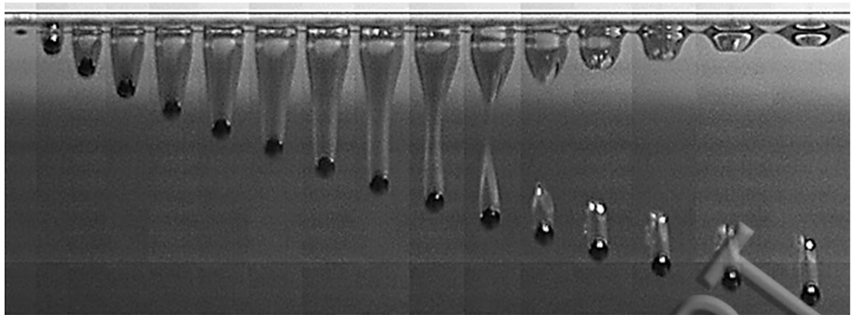

Figure 7: Figure 27 from Tan (2016). Deep seal observed after a steel sphere (D = 8 mm, u_i = 2.8 m/s) submerged in a deep pool of sunflower oil. The sphere created a long cavity at its wake which split into two at a depth about half of that of the sphere. An upward jet was being ejected from the surface despite not being visible in the images. The time difference between each successive image is 4 ms.

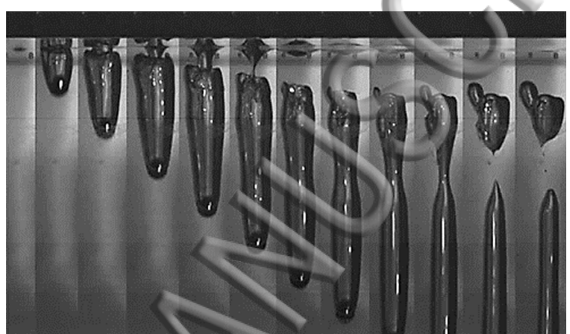

Figure 8: Figure 28 from Tan (2016). Deep seal and shallow seal observed following the entry of a steel sphere (D = 7 mm and u_i = 3.96 m/s) into sunflower oil. The cavity expanded while being dragged into the oil. The time difference between each successive image is 4 ms.

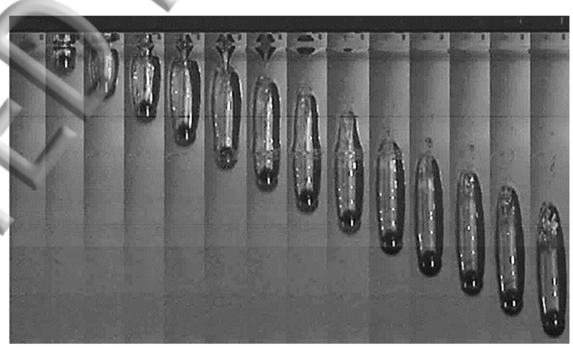

Figure 9: Figure 29 from Tan (2016). Shallow seal observed following the entry of a steel sphere (D = 8 mm, u_i = 4.64 m/s) into sunflower oil. The cavity pinched off immediately underneath the surface at about 12 ms after sphere entry, resulting in the formation of a relatively small cavity. The time difference between each successive image is 2 ms.

Figure 10: Figure 30 from Tan (2016). Another example of the shallow seal. The sphere (D = 8 mm, u_i = 5.6 m/s) created a smaller cavity than in Figure 9 that pinched off about 5 ms after sphere entry. The deep seal did not occur while a jet of oil ejected from the surface. The time difference between each successive image is 2 ms.

As presented in Figures 9 and 10, the appearance and phenomenon of shallow seal was very similar to those of the deep seal. The upper cavity subsequent to the pinch-off, collapsed rapidly towards the surface, producing a thin, upward oil jet. This jet however, due to lower pressure, would be thinner and would potentially reach a lower height compared to the jet generated during the deep seal.

The shallow seal transition velocity, u_{ss} and the shallow seal time, t_{ss} as defined in Section 3.1, were being measured. It was found that for spheres of a common diameter, D, the u_{ss} for sphere entries into both pure sunflower oil and the two-layer sunflower oil-water system were identical. This observation supports the hypothesis that the 'unusual' shallow seal phenomenon written in Section 3.1 had originated from the thin layer of sunflower oil that was resting on the water surface.

In addition, the deep seal disappearance velocity, u_{dd}, defined as the impact velocity above which the deep seal no longer occurs and the shallow seal depth, y_{ss}, defined as the vertical distance between the pinch-off point and the oil surface, were also measured. Multiple repeated experiments showed that the u_{dd} was consistent for spheres with a common diameter, D suggesting that the phenomenon where the deep seal stops occurring is also dependent on the inertia of the solid body.

Using u_{ss} and u_{dd} for the calculation of the Bond number, Bo and Weber number, We for spheres of each diameter used in the present study, a regime diagram similar to that shown in Figure 5 is presented in Figure 11.

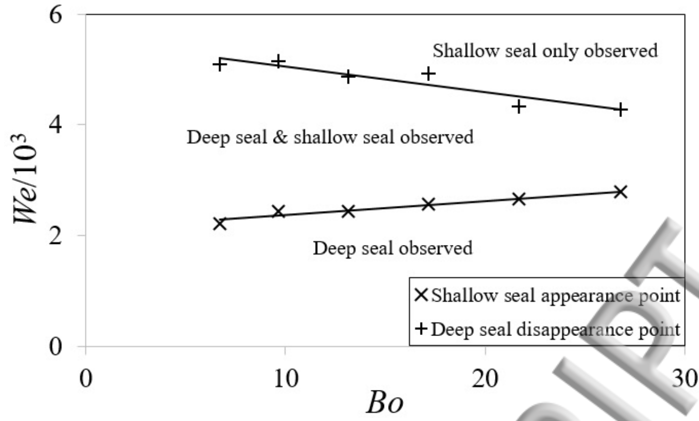

Figure 11: A regime diagram showing the different cavity sealing phenomena observed with respect to the Bond number, *Bo* and Weber number, *We*. The 'shallow seal appearance point' and 'deep seal disappearance point' was calculated using the shallow seal transition velocity, u_{ss} and the deep seal disappearance velocity, u_{dd} respectively. Both u_{ss} and u_{dd} were found to be dependent on the sphere diameter, suggesting a relationship between the generation of the different cavity sealing phenomena and the sphere inertia.

Figure 11 shows the three different cavity sealing phenomena observed with respect to the Bond number, *Bo* and Weber number, *We*. The 'shallow seal appearance point' and the 'deep seal disappearance point' were calculated for each sphere diameter, *D* using the u_{ss} and u_{dd} respectively. It can be concluded that the larger the diameter of the sphere, the lower velocity is required to generate the 'shallow seal only' phenomenon. Meanwhile, the 'deep seal observed' phenomenon is graphically presented in Figure 7, the 'deep seal & shallow seal observed' in Figure 8 and the 'shallow seal only observed' in Figures 9 and 10.

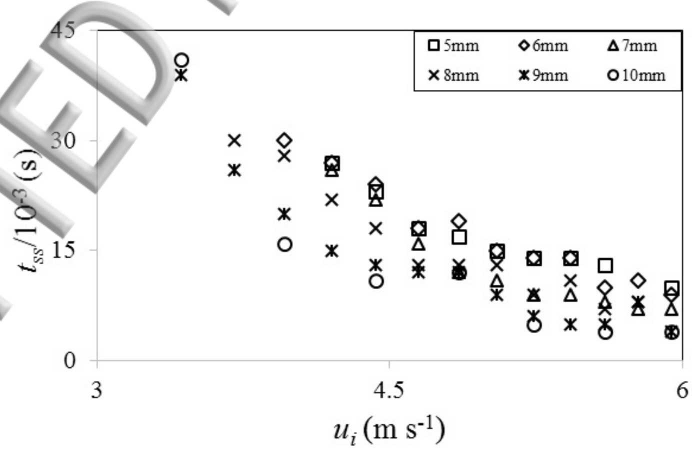

Figure 12: The shallow seal time, t_{ss} as a function of the impact velocity of the spheres, u_i. The diameters of the spheres are shown in the legend.

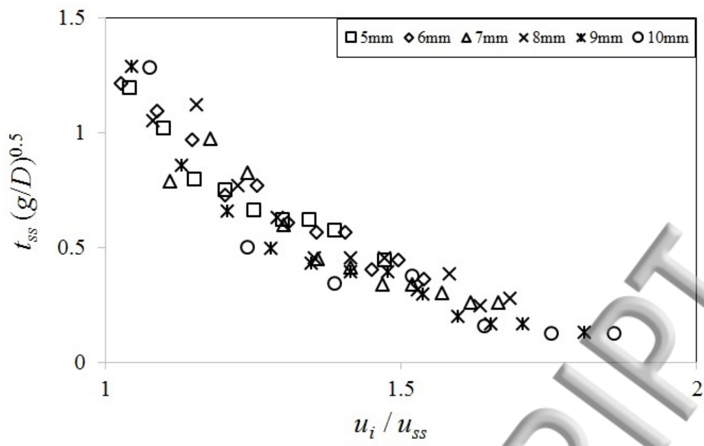

Figure 13: The non-dimensional shallow seal time, $t_{ss}\,(g/D)^{0.5}$ as a function of the non-dimensional impact velocity of the spheres, u_i / u_{ss}. The data confirms the dependence of t_{ss} on the inertial forces of the spheres. The diameters of the spheres are shown in the legend.

Figure 12 presents the shallow seal time, t_{ss} as a function of the impact velocity of the spheres, u_i. The data show that shallow seal occurred earlier at higher impact velocity and with larger spheres, suggesting a possible dependence on the inertial forces of the spheres. As written earlier, a consequence of a shorter t_{ss} would be the formation of relatively smaller cavities as shown in Figure 10.

Figure 13 presents the relationship between the non-dimensional shallow seal time, $t_{ss}\,(g/D)^{0.5}$ and the non-dimensional impact velocity of the spheres, u_i / u_{ss}. The data suggest that the non-dimensional shallow seal time scales approximately with the non-dimensional impact velocity by a factor of power -2. The results therefore, confirm the dependence of t_{ss} on the inertial forces of the spheres.

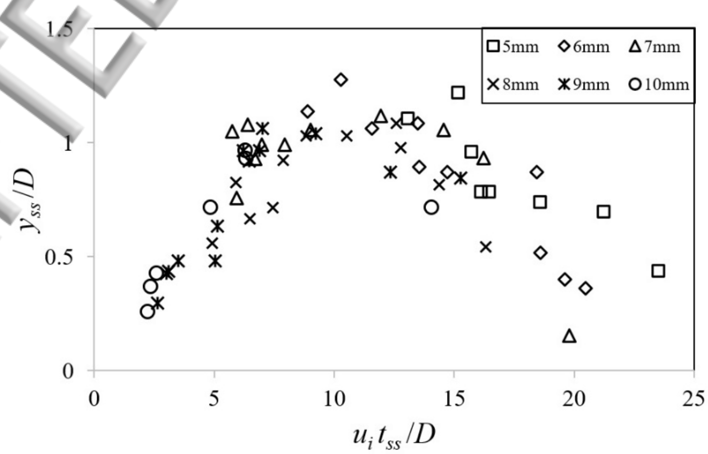

Figure 14: The non-dimensional shallow seal depth, y_{ss}/D as a function of the non-dimensional ideal sphere depth during shallow seal, $u_i\,t_{ss}$ /D. The diameters of the spheres are shown in the legend.

Meanwhile, Figure 14 presents the relationship between the non-dimensional shallow seal depth, y_{ss}/D and the non-dimensional ideal sphere depth during shallow seal, $u_i\ t_{ss}/D$. The viscous effects on sphere dynamics have been neglected since the actual sphere depth is not the focus of study at this point. As the decrease in t_{ss} was more significant than the increase in u_i in the calculation of the ideal sphere depth, the data in Figure 14 show that as u_i increases, shallow seal would occur closer to the oil surface. Figure 14 also shows that shallow seal would occur at a depth less than 1.5 times the diameter of the submerging sphere.

Since the shallow seal occurred at a depth very close to the surface, it would be worth discussing the influence of the surface tension of sunflower oil on the generation of the aforementioned shallow seal. The capillary length, $l_c = (\sigma / \rho g)^{0.5}$ of sunflower oil was calculated to be 1.93 mm. However, the experimental data for y_{ss} show 1.09 mm $\leq y_{ss} \leq$ 9.64 mm with all but 2 data values greater than the capillary length. Meanwhile, as shown in Figure 11, the Weber and Bond numbers in the present experiments were in the order of 1000 and 10 respectively, suggesting that surface tension was insignificant compared to the inertial forces of the spheres. Therefore, it can be concluded that the surface tension of sunflower oil had limited or even insignificant influence on the generation of the shallow seal observed.

The normal shallow seal described in the literature is a consequence of capillary instability and from the above analysis, it is logical to conclude that the 'unusual' shallow seal observed in the present investigation is of a different nature. Therefore, it is not surprising that the cavity sealing phenomena and their order of occurrences presented in this section and Section 3.1 are different to those documented in the existing literature (for example: Aristoff & Bush (2009) and Truscott *et al.* (2014)).

Meanwhile, a reasonable explanation for the generation of the 'unusual' shallow seal would be the surface conditions of the submerging spheres. This hypothesis is supported by Worthington (1908) and May (1951) who discovered that the surface conditions of a submerging solid body has a direct influence on the minimum impact velocity required for cavity generation after liquid entry.

In order to verify this hypothesis, similar sunflower oil entry experiments were performed using the same steel spheres. However, in this new set of experiments, the steel spheres were first immersed in sunflower oil itself before being cleaned by a tissue paper prior to each entry into the deep pool of sunflower oil. This additional procedure gave the spheres an oily surface without an obvious or significant oil film coating them.

The new sets of experiments involving 'oily' spheres generated surface seal – a phenomenon that was not observed during the previous sets of experiments. In addition, the order of the different cavity sealing phenomena generated with respect to increasing impact velocities and diameters as presented in Aristoff & Bush (2009) were also reproduced. It is important to note that in the new sets of experiments, the 'unusual' phenomena, namely the shallow seal that occurred at relatively high impact velocities and the complete absence of the deep seal at higher impact velocities, were not being observed. Meanwhile, a detailed regime diagram was not produced since the oily sphere experiments was not the subject of the present study and therefore, not investigated in greater detail.

Therefore, it is reasonable to conclude that the 'unusual' phenomena observed in Sections 3.1 and 3.2 were a result of the surface conditions of the spheres relative to the sunflower oil they entered.

4. Conclusion

The primary objective of this paper is to experimentally demonstrate the significant influence a thin upper layer liquid can potentially have, on the cavity dynamics and phenomena observed subsequent to the entry of solid bodies into a stratified, two-layer system of immiscible liquids.

Tan *et al.* (2016) had identified the significant effects a thin viscous oil layer has on the dynamics of spheres entering into a stratified, two-layer oil-water system. The drag coefficients were found to have increased by up to 250 % for smaller steel spheres (D = 5 mm) when a 5 mm layer of silicone oil (ν_o = 1000 mm^2/s) was present on the surface of the deep pool of water. Meanwhile, the average velocity at the instant of deep seal was found to decrease by approximately 5 % and 20 % when the water was covered by a 5 mm layer of sunflower oil and a 5 mm layer of the aforementioned silicone oil respectively.

In Section 3.1, 'unusual' shallow seal (cavity pinching off close to the liquid surface) had been observed following the entry of steel spheres at relatively high velocity into a two-layer, sunflower oil-water system. Further increases in the impact velocity of the spheres led to the shallow seal occurring almost immediately after sphere entry, resulting in the formation of relatively small cavities that did not experience deep seal (cavity pinching off at a significant depth below the liquid surface). These observations have never been documented in the literature and therefore, they represent a new finding and understanding on the subject.

In Section 3.2, experimental investigations revealed that the phenomena in Section 3.1 were generated as a result of the surface conditions of the steel spheres with respect to the sunflower oil. As the oil layer was relatively thin compared to the dimensions of the spheres (oil layer thickness was 5 mm while the diameter of the spheres was between 2.9 mm and 14.3 mm), the results highlighted the significant influence even a very thin oil layer could have. In addition, the 'unusual' shallow seal observed were found to be of a different nature relative to the normal shallow seal described in the literature such as in Aristoff & Bush (2009) and Truscott *et al.* (2014). Further investigations also highlighted and increased current understanding on the substantial influence the surface conditions of the submerging body could have, on cavity formations and dynamics that were mentioned by Worthington (1908) over a century ago.

It is thought that the steel spheres might generate significant cavities again should they enter sunflower oil at higher impact velocities. However, due to limitations of the laboratory conditions, it was not possible to verify this hypothesis during the present study.

References

Akers B. and Belmonte A., ''Impact dynamics of a solid sphere falling into a viscoelastic miscellar fluid'', *J. Non-Newtonian Fluid Mech.* **135**, 97-108 (2006)

Aristoff J. M. and Bush J. W. M., ''Water entry of small hydrophobic spheres'', *J. Fluid Mech.* **619**, 45-79 (2009)

Franklin B., Brownrigg W. and Rev. Mr Farish, ''Of the Stilling of Waves by means of Oil'', *Phil. Trans* **64**, 445-460 (1774)
(Web: http://rstl.royalsocietypublishing.org/content/64/445. Last accessed: 22 May 2018)

Gekle S., Gordillo J. M., van der Meer D. and Lohse D., ''High Speed Jet Formation after Solid Object Impact'', *Phys. Rev. Lett.* **102**, 034502 (2009)

Gekle S., Peters I. R., Gordillo J. M., van der Meer D. and Lohse D., ''Supersonic Air Flow due to Solid-Liquid Impact'', *Phys. Rev. Lett.* **104**, 024501 (2010)

Gekle S. and Gordillo J. M., ''Generation and Breakup of Worthington jets after cavity collapse. Part 1. Jet formation'', *J. Fluid Mech.* **663**, 293-330 (2010)

Gordillo J. M. and Gekle S., ''Generation and Breakup of Worthington jets after cavity collapse. Part 2. Tip breakup of stretched jets'', *J. Fluid Mech.* **663**, 331-346 (2010)

Lee M, Longoria R. G. and Wilson D. E., ''Cavity dynamics in high-speed water entry'', *Phys. Fluids* **9**, 540-550 (1997)

Le Goff A., Quere D. and Clanet C., ''Viscous cavities'', *Phys. Fluids* **25**, 043101 (2013)

May A., ''Effect of Surface Conditions of a Sphere on its Water Entry Cavity'', *J. Appl. Phys.* **22**, 1219-1222 (1951)

May A., ''Vertical Entry of Missiles into Water'', *J. Appl. Phys.* **23**, 1362-1372 (1952)

Peters I. R., van der Meer D. and Gordillo J. M., ''Splash wave and crown breakup after disc impact on a liquid surface'', *J. Fluid Mech.* **724**, 553-580 (2013)

Tan B. C.-W., Ph.D. Thesis, University of Warwick, UK (2016)
(Web: http://wrap.warwick.ac.uk/84842/1/WRAP_Theses_Tan_2016.pdf. Last accessed: 6 March 2018)

Tan B. C.-W., Vlaskamp J. H. A., Denissenko P. and Thomas P. J., ‘‘Cavity formation in the wake of falling spheres submerging into a stratified two-layer system of immiscible liquids’’, *J. Fluid Mech* **790**, 33-56 (2016)

Truscott T. T., Epps B. P. and Belden J., ‘‘Water Entry of Projectiles’’, *Ann. Rev. Fluid Mech.* **46**, 355-378 (2014)

Worthington A. M., ‘‘On Impact with a Liquid Surface’’, *Proc. R. Soc. Ser. A* **34**, 217-230 (1882)

Worthington A. M., *A Study of Splashes*, Longmans, Green and co., London, UK (1908)

Worthington A. M. and Cole R. S., ‘‘Impact on a liquid surface studied by the aid of instantaneous photography’’, *Phil. Trans. R. Soc. Ser. A* **189**, 137-148 (1897)

Worthington A. M. and Cole R. S., ‘‘Impact on a liquid surface studied by the aid of instantaneous photography, Paper II’’, *Phil. Trans. R. Soc. Ser. A* **194**, 175-199 (1900)


oil layer
deep seal
water

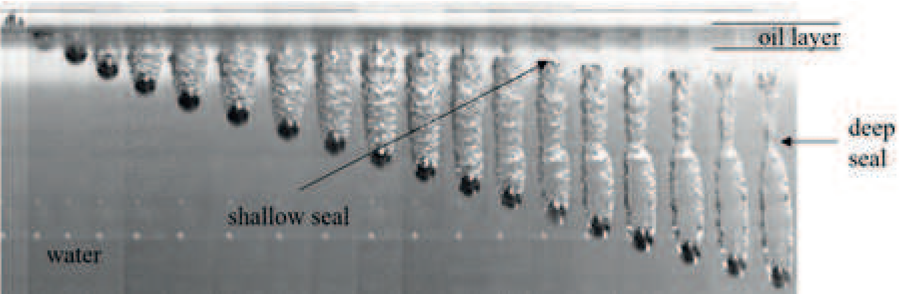
oil layer
deep
seal
shallow seal
water


oil layer
oil trail
shallow seal
water


oil layer
oil trail
vortex cloud
shallow seal
water

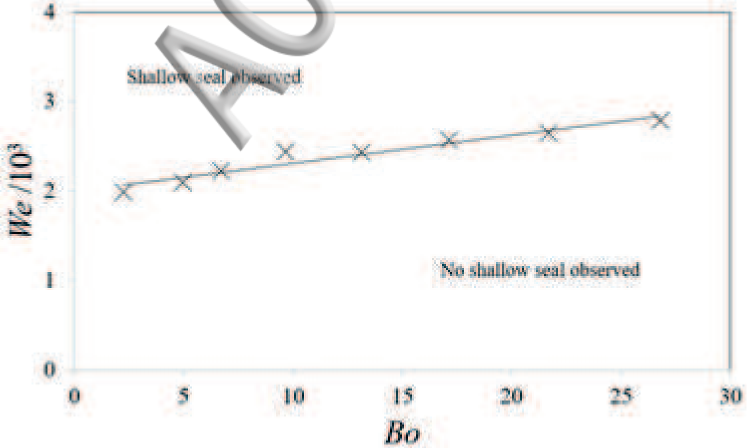
Shallow seal observed
No shallow seal observed
We /10^3
Bo
0
1
2
3
4
0
5
10
15
20
25
30

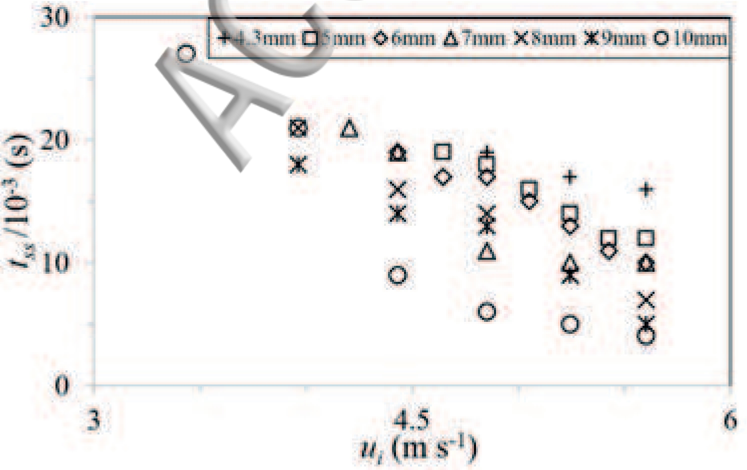

+4.3mm □5mm ◇6mm △7mm ×8mm ✱9mm ○10mm
30
20
10
0
3
4.5
6
t_{ss}/10^{-3} (s)
u_t (m s^{-1})

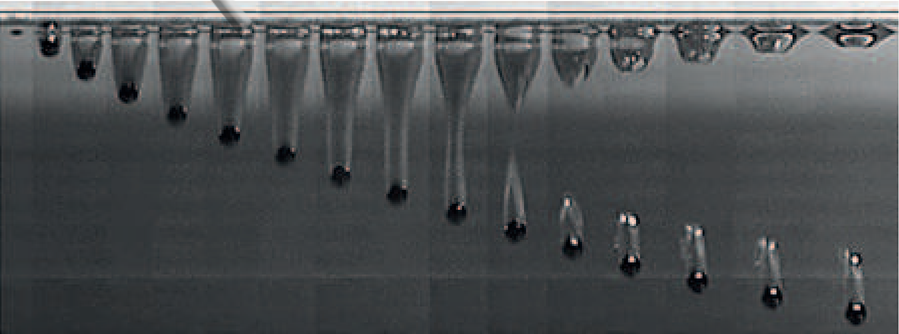

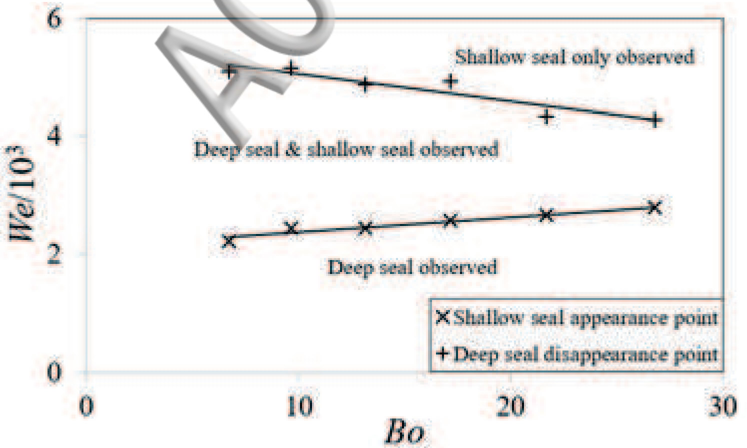

Shallow seal only observed
Deep seal & shallow seal observed
Deep seal observed
Shallow seal appearance point
Deep seal disappearance point
$We/10^3$
Bo
0
2
4
6
0
10
20
30

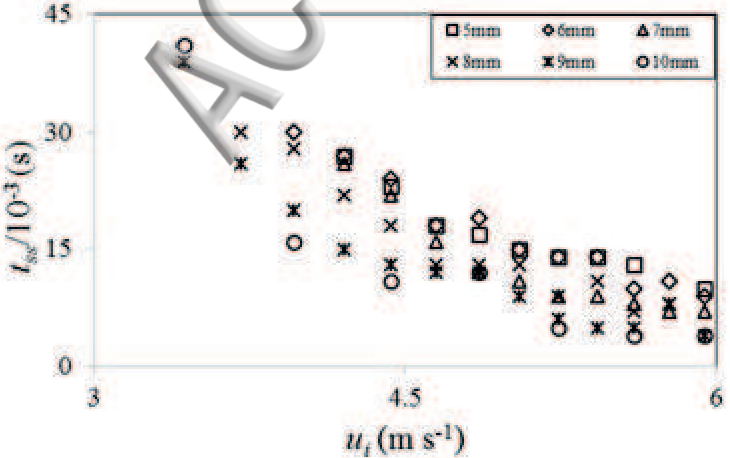
5mm
6mm
7mm
8mm
9mm
10mm
45
30
15
0
3
4.5
6
$t_{su}/10^{-3}$(s)
u_t (m s^{-1})

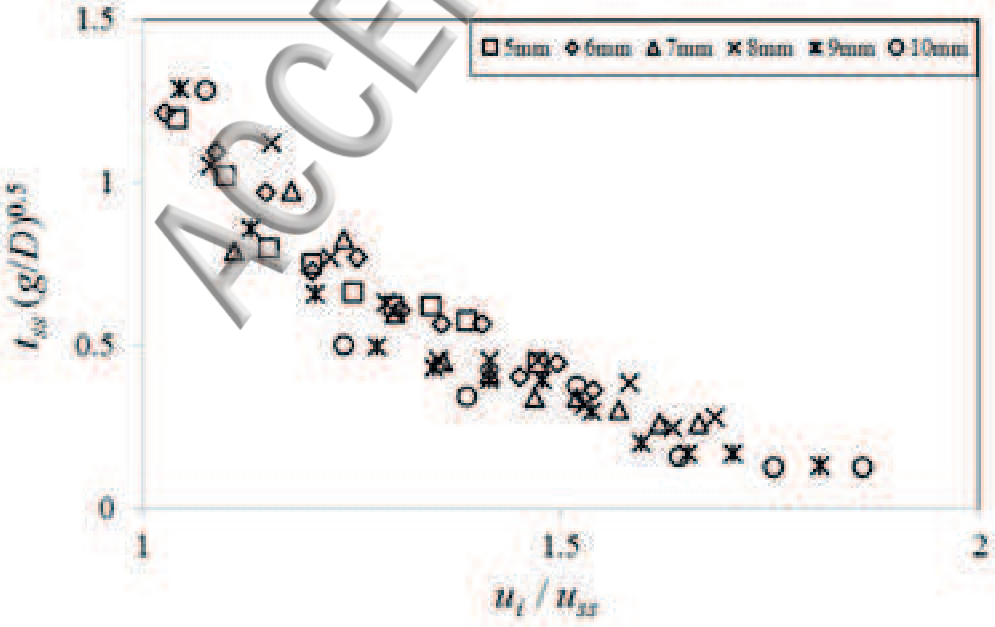
5mm
6mm
7mm
8mm
9mm
10mm
1.5
1
0.5
0
1
1.5
2
$t_{sw}\,(g/D)^{0.5}$
$u_t\,/\,u_{ss}$

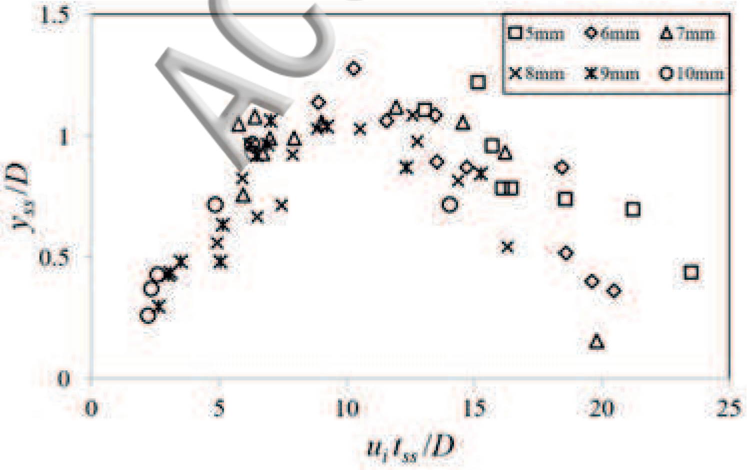
5mm
6mm
7mm
8mm
9mm
10mm
1.5
1
0.5
0
0
5
10
15
20
25
y_{ss}/D
$u_i t_{ss}/D$